

# Macrocyclic Metal Complexes for Metalloenzyme Mimicry and Sensor Development

Published as part of the Accounts of Chemical Research special issue "Synthesis in Biological Inorganic Chemistry".

Tanmaya Joshi,<sup>\*,†</sup> Bim Graham,<sup>\*,‡</sup> and Leone Spiccia<sup>\*,†</sup>

<sup>†</sup>School of Chemistry, Monash University, Victoria 3800, Australia

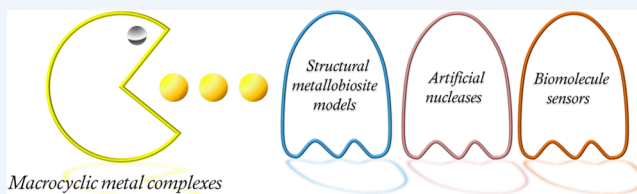
<sup>‡</sup>Monash Institute of Pharmaceutical Sciences, Monash University, Parkville, Victoria 3052, Australia

**CONSPECTUS:** Examples of proteins that incorporate one or more metal ions within their structure are found within a broad range of classes, including oxidases, oxidoreductases, reductases, proteases, proton transport proteins, electron transfer/transport proteins, storage proteins, lyases, rusticyanins, metallochaperones, sporulation proteins, hydrolases, endopeptidases, luminescent proteins, iron transport proteins, oxygen storage/transport proteins, calcium binding proteins, and monooxygenases. The metal coordination environment therein is often generated from residues inherent to the protein, small exogenous molecules (e.g., aqua ligands) and/or macrocyclic porphyrin units found, for example, in hemoglobin, myoglobin, cytochrome C, cytochrome C oxidase, and vitamin B<sub>12</sub>. Thus, there continues to be considerable interest in employing macrocyclic metal complexes to construct low-molecular weight models for metallobiosites that mirror essential features of the coordination environment of a bound metal ion without inclusion of the surrounding protein framework.

Herein, we review and appraise our research exploring the application of the metal complexes formed by two macrocyclic ligands, 1,4,7-triazacyclononane (tacn) and 1,4,7,10-tetraazacyclododecane (cyclen), and their derivatives in biological inorganic chemistry. Taking advantage of the kinetic inertness and thermodynamic stability of their metal complexes, these macrocyclic scaffolds have been employed in the development of models that aid the understanding of metal ion-binding natural systems, and complexes with potential applications in biomolecule sensing, diagnosis, and therapy. In particular, the focus has been on "coordinatively unsaturated" metal complexes that incorporate a kinetically inert and stable metal–ligand moiety, but which also contain one or more weakly bound ligands, allowing for the reversible binding of guest molecules via the formation and dissociation of coordinate bonds.

With regards to mimicking metallobiosites, examples are presented from our work on tacn-based complexes developed as simplified structural models for multimetallic enzyme sites. In particular, structural comparisons are made between multinuclear copper(II) complexes formed by such ligands and multicopper enzymes featuring type-2 and type-3 copper centers, such as ascorbate oxidase (AO) and laccase (Lc). Likewise, with the aid of relevant examples, we highlight the importance of cooperativity between either multiple metal centers or a metal center and a proximal auxiliary unit appended to the macrocyclic ligand in achieving efficient phosphate ester cleavage. Finally, the critical importance of the Zn(II)–imido and Zn(II)–phosphate interactions in Zn–cyclen-based systems for delivering highly sensitive electrochemical and fluorescent chemosensors is also showcased.

The Account additionally highlights some of the factors that limit the performance of these synthetic nucleases and the practical application of the biosensors, and then identifies some avenues for the development of more effective macrocyclic constructs in the future.



## INTRODUCTION

Numerous proteins incorporate metal ions within their structure. In most cases, the metal coordination environment is generated from residues present within the protein, often in combination with small exogenous molecules. In biological molecules such as cytochrome C and hemoglobin, however, the metal ions are bound by porphyrins. The metal ion-ligating environments found within biological systems can be broadly divided into two classes: (1) cases where the metal ion coordination sphere is "saturated" or remains unchanged during function and (2) cases where ligand exchange is critical to

function. For both classes, considerable efforts have been made to understand the purpose and operation of natural systems by accessing synthetic metal complexes that mimic the structure or function of the active sites. In addition, metal complexes have become important targets in the development of sensors, diagnostic agents, biomolecule separation tools, and therapeutic agents. For these purposes, a plethora of acyclic and macrocyclic ligands have been employed.<sup>1–9</sup> In comparison

Received: March 23, 2015

Published: August 5, 2015

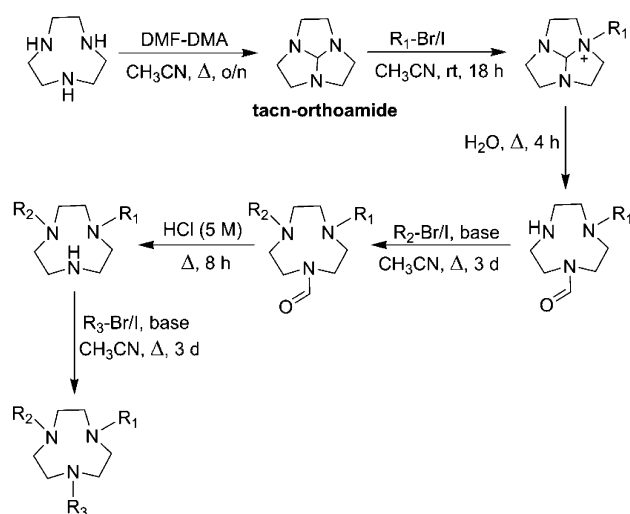
to acyclic ligands, macrocyclic ligands form metal complexes with higher kinetic inertness and thermodynamic stability owing to the so-called “macrocyclic effect”.<sup>10</sup> Consequently, they are attractive scaffolds for assembling metal complexes for a multitude of applications. In our studies, two macrocyclic ligands, 1,4,7-triazacyclononane ([9]aneN<sub>3</sub>, tacn) and 1,4,7,10-tetraazacyclododecane ([12]aneN<sub>4</sub>, cyclen), have proven instrumental in efforts to advance the understanding of metal ion-binding biological systems and to develop systems with potential practical applications. In this Account, we highlight the utility of these macrocycles and their derivatives by discussing examples from our own studies and then place this research into a broader perspective by comparing our findings with those of others in the field. We focus on “coordinatively unsaturated” metal complexes, in which binding of the macrocycle results in complexes that combine a kinetically inert and thermodynamically stable metal–ligand moiety with one or more weakly bound ligands that can be used to confer particular properties or functions to the complex. As in studies by others in the field of biological inorganic chemistry, the intention is to mimic important functional properties of biological systems and to exploit them for emerging applications in chemistry, biology, and medicine.

## ■ STRUCTURAL METALLOBIOSITE MODELS

Tacn and its derivatives are ideally suited to generating mono- and polynuclear metal complexes, since tacn is a tridentate ligand that coordinates facially to a metal ion, leaving two or three coordination sites available for attaching substrate molecules or for bridge formation.<sup>10</sup> Versatile synthetic methodology has allowed access to a wide array of functionalized tacn derivatives, which have proven useful for generating metalloenzyme structural models.<sup>1</sup> In this regard, “tacn-orthoamide”<sup>11,12</sup> has been extensively used to access symmetric and asymmetric ligands containing a variety of coordinating pendant groups (Scheme 1), as well as ligands featuring multiple linked tacn rings (Figure 1).<sup>13–15</sup>

A major focus of our work has been on new tacn-based ligands capable of generating structural models for copper protein active sites.<sup>16–28</sup> The metal centers within copper proteins generally reside in sites generated by four or five

**Scheme 1. Synthetic Route to Asymmetrically-Functionalized Tacn-Based Ligands**



metal-coordinating residues, with the coordination sphere completed by aqua ligands and/or substrate donor atoms. For example, histidine residues bind to copper ions in the mono-, di-, or trinuclear Cu(II) sites of hemocyanin, ceruloplasmin, dicopper dismutase, galactose oxidase, catechol oxidase, and quercetin 2,3-dioxygenase.<sup>29</sup> Given the high affinity of tacn for Cu(II), it is a good mimic for metal-binding sites generated by histidine residues.<sup>1,30</sup>

As simplified model compounds of relevance to multicopper enzymes, such as ascorbate oxidase (AO) and laccase (Lc), we investigated tri-, tetra-, and hexanuclear Cu(II) complexes of tacn-based ligands **14** and **15** (Figure 1).<sup>18,22–24,26</sup> Multicopper oxidases generally contain three types of copper centers, termed type-1, type-2, and type-3. The type-2 and type-3 centers form a trinuclear cluster bridged by exogenous ligands.<sup>29</sup> In order to mimic the Cu(II) coordination environment of these enzymes, model complexes were rationally designed to hold three or more Cu(II) centers in close proximity and in a specific spatial arrangement, to allow study of Cu···Cu interactions over short distances. Depending on the M/L ratio, solution pH, and presence of additional ligands, we found that the tri- and tetra-macrocyclic ligands formed tri-, tetra-, and hexanuclear complexes, including species featuring exogenous hydroxo, azido, phosphate, and alkoxy bridges (examples shown in Figure 2).<sup>18,22–24,26</sup>

In addition to the metal–metal separation, metal–metal interactions in hydroxo- and alkoxy-bridged multinuclear complexes are influenced by the M–O(bridge) distances, the M–O–M angle, the dihedral angle between planes of the Cu(OH)<sub>2</sub> or Cu(OR)<sub>2</sub> units, the out-of-plane displacement of the bridging groups, and the Cu(II) geometry. In our studies, magnetic susceptibility measurements showed the existence of weak antiferromagnetic coupling for bridged complexes featuring “roof-shaped” Cu(II)<sub>2</sub>(μ<sub>2</sub>-OH)<sub>2</sub> cores ( $J \approx -30$  cm<sup>-1</sup>), and strong coupling for those with Cu(II)<sub>2</sub>(μ<sub>2</sub>-OMe)<sub>2</sub> cores ( $J \approx -270$  cm<sup>-1</sup>).<sup>18,22–24,26</sup> In contrast, the μ-1,1 end-on azido-bridged complex showed ferromagnetic coupling ( $J = 94$  cm<sup>-1</sup>), which was attributed to the lower electronegativity of the azide ligand.<sup>23</sup>

In terms of their relevance to multicopper enzymes, such multinuclear complexes can be viewed as “self-assembling” constructs featuring multiple type-2 and type-3 copper centers.<sup>26</sup> In the [Cu<sub>3</sub>-**14**(μ-OH)(μ<sub>3</sub>-HPO<sub>4</sub>)(H<sub>2</sub>O)]<sup>3+</sup> complex shown in Figure 3, the trinuclear sites consist of two type-3 Cu(II) centers, (Cu(1), Cu(2)) linked by one hydroxo and two phosphate oxygens, and a type-2 Cu(II) center (Cu(3)) linked to them by another phosphate oxygen.<sup>26</sup> These sites exhibit structural similarities to the active sites of AO and Lc. In our model, the separation between two type-3 copper centers (3.557(4) Å) and their distance from the type-2 center (4.561(4) and 5.474(4) Å) are longer than those in the trinuclear copper sites of AO (Figure 4). However, they match those of azido- and peroxo-modified AO, where the type 3–type 3 and two type 2–type 3 copper separations are 5.1 (4.8 for peroxo-) Å, 3.6 (4.5 for peroxo-) Å, and 4.6 (3.7 for peroxo-) Å, respectively (Figure 4).<sup>31</sup> The solution ESR spectrum was also similar to those of Lc and AO, with the type-3 Cu(II) centers being ESR silent. It is important to note the effect of the structure of the trinuclear sites on the in-solution physical properties. For instance, magnetic and ESR data for our model complex were different from those of the oxidized Lc or AO. This can be explained on the basis of differences in the bridges connecting the copper centers, namely, the type-3 Cu–(OH)–

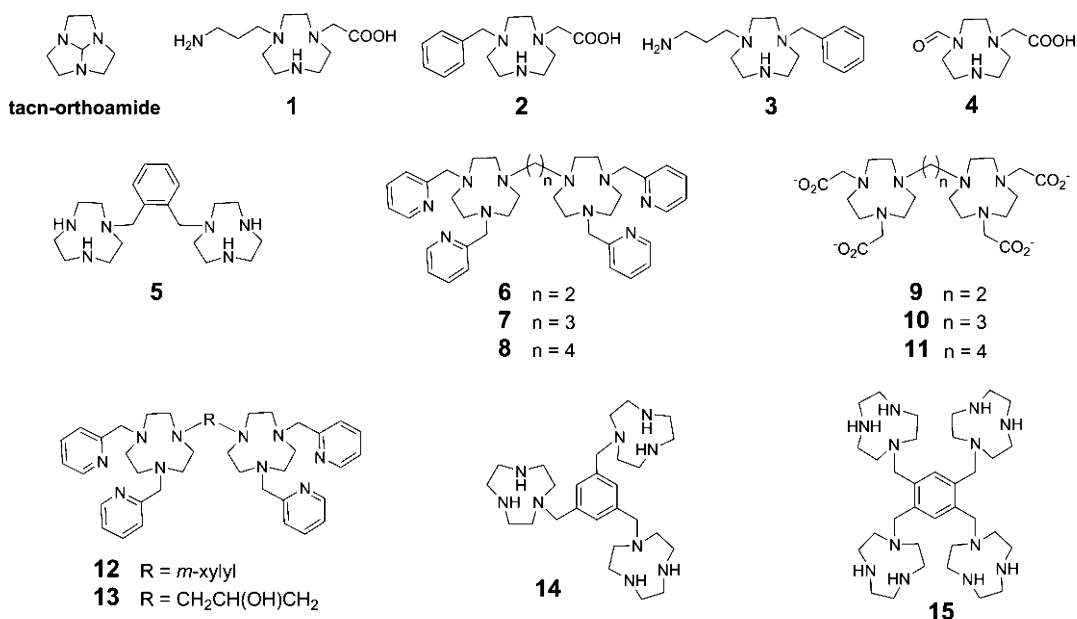


Figure 1. Tacn-based ligands used to develop metalloprotein models.

Cu and Cu(type-3)–O(OH)–Cu(type-2) bridges in the oxygen intermediate of the native enzyme vs a hydroxo and a phosphate-based bridge in the complex.

In general, in-solution organization of such assemblies can be induced by selecting sterically demanding ligands, in a manner similar to the multimetal clusters in metalloproteins. Inter-metallic distances of 3.5–4 Å are generally observed for hydroxy-bridged triangular Cu<sub>3</sub> complexes. This distance can be reduced by introducing an endogenous bridging group, such as a phenoxide.<sup>33</sup> A Cu⋯Cu separation of 3.11 Å was reported for the azido-bridged Cu(II) centers in Cu(II)<sub>3</sub>–17, with the third copper atom being ca. 7.5 Å away (Figure 5).<sup>33</sup> In the imidazolate-bridged Cu(II)<sub>3</sub>–21 complex, the metal centers are approximately at the corners of an equilateral triangle, and the Cu⋯Cu separations are ~5.92 Å,<sup>34</sup> whereas an asymmetric site was found in the acetate-bridged Cu(II)<sub>3</sub>–20 complex, namely, Cu⋯Cu distances of 3.198, 4.568, and 6.277 Å (Figure 5).<sup>35</sup> Another structural mimic of the AO active site is the trinuclear complex of a Schiff-base ligand, Cu(II)<sub>3</sub>–18 (Figure 5).<sup>32</sup> Like our phosphate-bridged Cu(II) complex, this complex features two type-3 Cu(II) centers, which lie 3.6 Å apart and are separated from the nonbridged type-2 center by 4.9 and 5.9 Å. Again, these distances are longer than those in the natural AO site. Even though these complexes are inexact active site models, due to their dissimilar Cu(II) coordination geometry and longer M⋯M separation, they nonetheless provide insights into some of the key structural and electronic features of the biosite.

Cu(II)<sub>3</sub>–23 is another tacn-based Cu(II) cluster in which a central μ<sub>3</sub>-HPO<sub>4</sub><sup>2-</sup> group bridges the metal centers (Figure 5).<sup>36</sup> However, in contrast to the [Cu<sub>3</sub>–14(μ-OH)(μ<sub>3</sub>-HPO<sub>4</sub>)(H<sub>2</sub>O)]<sup>3+</sup> complex reported by our group, this complex does not feature a secondary Cu–OH–Cu bridge. As a stabilized trimetal–phosphate cluster, Cu(II)<sub>3</sub>–23 is a discrete structural model for the trimetal active sites of phosphate-metabolizing enzymes (Figure 5). Likewise, despite the presence of different metal ions, the arrangement of the metal centers in the {[Cu<sub>3</sub>–14(μ-OH)(μ<sub>3</sub>-HPO<sub>4</sub>)(H<sub>2</sub>O)]<sup>3+</sup>}<sub>n</sub> polymer has close similarities to the trinuclear Zn(II)-containing active sites of phospholipase

C and P1 nuclease.<sup>37</sup> A key common feature is a hydroxo bridge between two metal centers (see Figures 4 and 6). The distance between the hydroxo-bridged zinc(II) centers (3.3 Å) and the corresponding copper(II) centers in our model are similar, as are the distances to the third distant metal ion (ca. 4.5 and 6.0 Å in phospholipase C and P1 nuclease and ca. 4.6 and 5.5 Å in the Cu(II) polymer).<sup>37</sup>

## ARTIFICIAL NUCLEASES

Interest in metal complexes that, like (ribo)nucleases and phosphatases, promote the hydrolysis of phosphate esters led us to explore coordinatively unsaturated cyclen and tacn metal complexes as mimics for such enzymes. Facile P–O bond hydrolysis and transesterification reactions are crucial for many biological processes. Many enzymes (protein-based as well as ribozymes) have evolved to accelerate these reactions by factors of 10<sup>15</sup> or more. In such enzymes, metal centers generally play pivotal roles in maintaining enzyme structural integrity, assisting with substrate binding and activation, delivering a metal bound-hydroxide as a highly reactive nucleophile, and/or stabilizing transition states and leaving groups.

Burstyn and co-workers, in their detailed mechanistic studies of the reaction between [Cu(tacn)(OH<sub>2</sub>)<sub>2</sub>]<sup>2+</sup> and activated model phosphodiester, such as bis(nitrophenyl)phosphate (BNPP), were first to recognize that tacn complexes hydrolyze phosphate esters (Scheme 2).<sup>1,41</sup> Following this work, several groups, including ours, developed Cu(II) complexes of N-alkylated tacn ligands that are more effective cleavage agents (Figure 7, Table 1).<sup>1,16,42–51</sup> For example, the rates of BNPP cleavage by the Cu(II)–Me<sub>3</sub>tacn and Cu(II)–<sup>i</sup>Pr<sub>3</sub>tacn complexes, Cu(II)–26 and Cu(II)–27, are ~100-fold faster.<sup>1,47</sup> Moreover, the cleavage of nitrophenylphosphate (NPP), the monoester product of BNPP hydrolysis, is also enhanced in some cases.

The mechanism of hydrolysis is postulated to involve deprotonation of [CuL(OH<sub>2</sub>)<sub>2</sub>]<sup>2+</sup> to form [CuL(OH<sub>2</sub>)(OH)]<sup>+</sup>, substrate coordination, and rate-determining phosphate ester cleavage (Scheme 2).<sup>41,48</sup> However, formation of the hydrolytically inactive [LCu(μ-OH)<sub>2</sub>CuL]<sup>2+</sup> complex, through

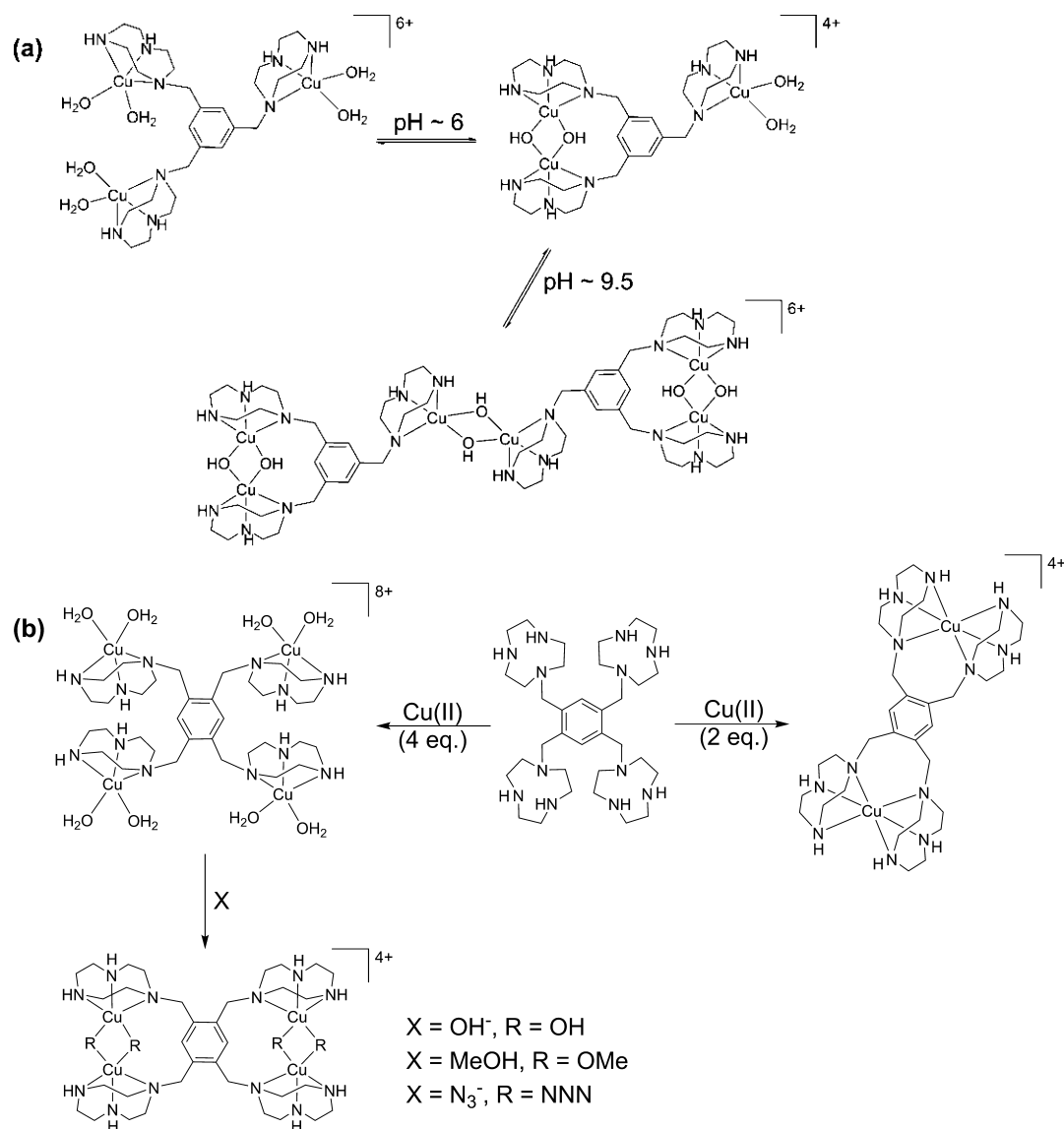


Figure 2. Cu(II) complexes formed by ligands 14 (a) and 15 (b).<sup>18,22–24,26</sup>

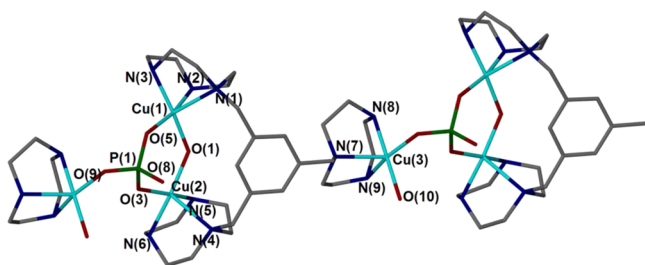


Figure 3. Phosphate-bridged  $\{[\text{Cu}_3\text{-14}(\mu\text{-OH})(\mu_3\text{-HPO}_4)(\text{H}_2\text{O})]^{3+}\}_n$  chains containing trinuclear Cu(II) sites. Adapted with permission from ref 26. Copyright 1997 Royal Society of Chemistry.

dimerization of  $[\text{CuL}(\text{OH}_2)(\text{OH})]^+$ , reduces the activity achievable by these complexes (Scheme 2). This dimer provides neither a site for substrate binding nor a coordinated nucleophile for attacking the substrate, since bridging hydroxides are poorer nucleophiles than water or terminal hydroxides. Importantly, the rate enhancements afforded by N-alkylation, attributable to reduced formation of the inactive

dimer, point to this being a viable method for improving the activity of these complexes.<sup>1</sup>

Interestingly, significant enhancements in reactivity in comparison to the Cu(II)–tacn complex were achieved with only two noncoordinating substituents on the tacn ring (Table 1). However, the choice of the pendant arm is critical. For example, in our studies, introduction of coordinating amino pendant arms rendered Cu(II)–33 and Cu(II)–34 inactive toward BNPP hydrolysis,<sup>45</sup> because fewer sites are available for complex–substrate interactions.

The fact that many hydrolytic metalloenzymes utilize multiple metal–substrate interactions for their catalytic activity has stimulated interest in multinuclear nuclease mimics. Seeking metal-ion cooperativity reminiscent of these enzymes, we have also investigated di- and trinuclear Cu(II) complexes of multi-tacn ligands (13 and 35–39, Figures 1 and 8).<sup>1,16,19,46,52</sup> While the *o*-xylyl bridged binuclear complex Cu(II)<sub>2</sub>–35 cleaves BNPP 25-times faster than Cu(II)–tacn (Cu(II)–24, Figure 7), the rate of cleavage was 100-fold higher for the trinuclear mesitylene-bridged complex Cu(II)<sub>3</sub>–13. The *m*-xylyl spacer in Cu(II)<sub>2</sub>–36, however, favors formation of

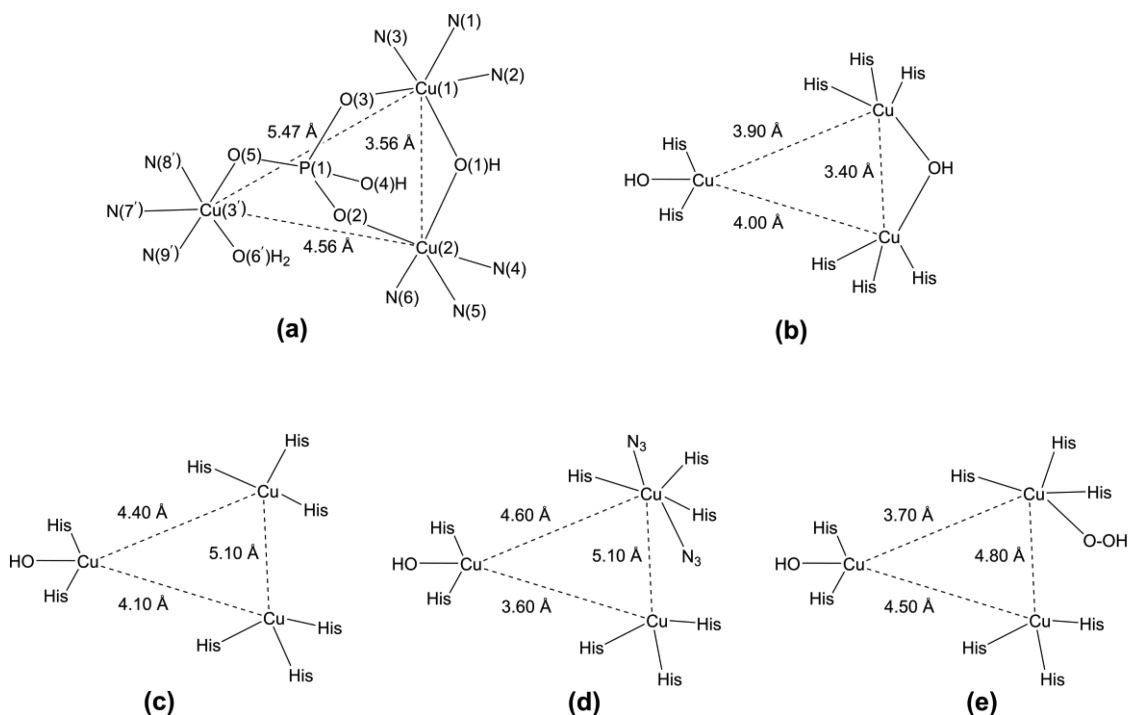


**Figure 4.** Comparison of trinuclear Cu(II) sites in (a) phosphate-bridged  $\{[\text{Cu}_3\text{-14}(\mu\text{-OH})(\mu_3\text{-HPO}_4)(\text{H}_2\text{O})]^{3+}\}_n$  polymer, (b) ascorbate oxidase (AO), (c) reduced form of AO; (d) azido-bound AO, and (e) peroxo-bound AO.<sup>26,31,32</sup>

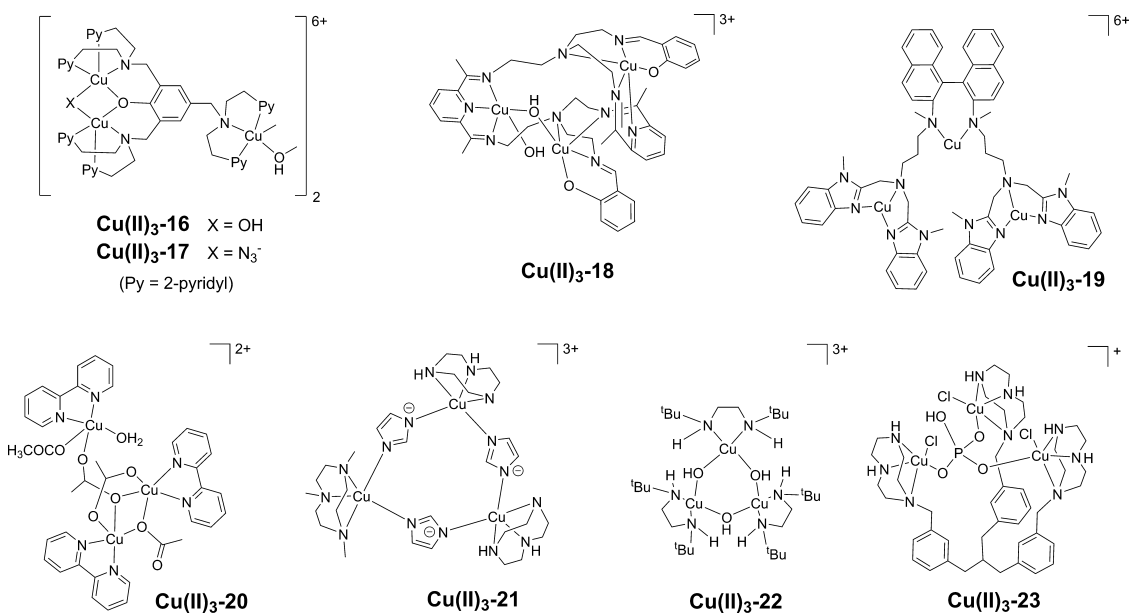


**Figure 5.** Examples of trinuclear Cu(II) complexes reported in the literature.<sup>32–36,38,39</sup>

inactive dihydroxo complexes, presenting reactivity similar to Cu(II)–24. Of note, a kinetic reaction of Cu(II)<sub>2</sub>–36 with BNPP afforded single crystals, whose analysis showed the formation of a NPP-bridged Cu(II) complex after BNPP cleavage to NPP (Figure 9).<sup>19</sup> This example highlights the importance of product release in sustaining a catalytic cycle. As for the mononuclear Cu(II) complexes, the cleavage rates of these binuclear complexes were further enhanced by N-methylation of the tacn rings (38 and 39, Figure 8).<sup>16</sup> As noted above, alkylation decreases the stability of inactive hydroxo-bridged binuclear complexes.

Arginine residues play key roles in promoting rapid phosphate ester hydrolysis in metalloenzymes, such as alkaline phosphatase (AP).<sup>1,52</sup> The positively charged guanidinium group in arginine is postulated to assist with substrate activation and transition state stabilization during the AP catalytic cycle through the formation of strong charge-assisted H-bonds.<sup>1</sup> Inspired by this, we developed tacn-guanidinium derivatives (40–47, Figure 8) to explore the possibility of improving cleavage activity.<sup>42–44</sup> It was hypothesized that cooperativity in phosphate ester cleavage could be achieved by having the Cu(II) center in close proximity to guanidinium groups,

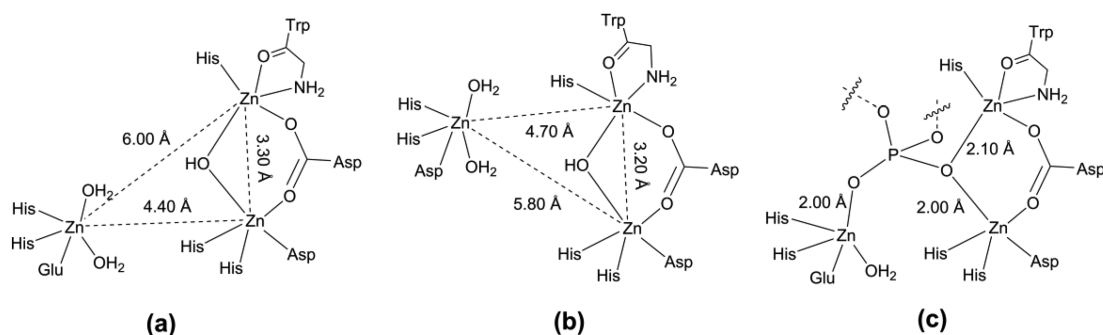


**Figure 6.** Trinuclear Zn(II) frameworks in the active sites of (a) phospholipase C, (b) P1 nuclease, and (c) inorganic phosphate ( $P_i$ )-bound phospholipase C.<sup>37,40</sup>

**Scheme 2. Proposed Mechanism for Phosphate Diester Hydrolysis by Cu(II)–Tacn Complexes<sup>41</sup>**

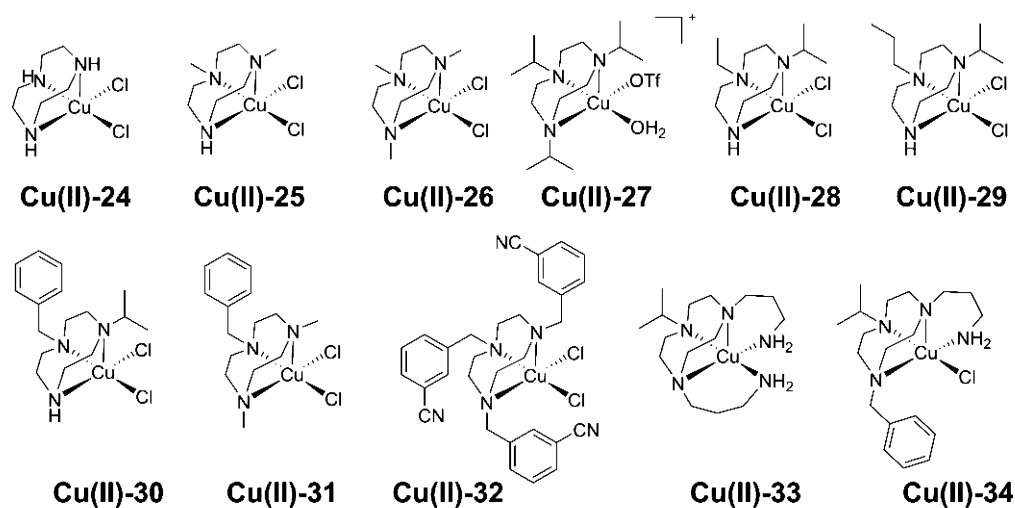
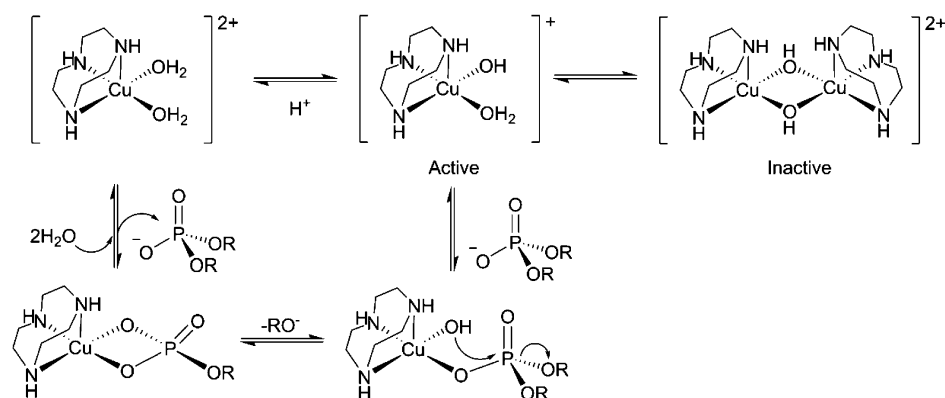


**Figure 7.** N-Substituted Cu(II)–tacn complexes applied in phosphate ester cleavage studies.<sup>1</sup>

thereby enhancing the cleavage of model phosphate esters and plasmid DNA.

When pairs of alkyl-guanidinium pendants were attached to the tacn backbone, only the propyl-guanidinium complex, Cu(II)–41, showed enhanced reactivity toward BNPP and HPNPP (2-hydroxypropyl-4-nitrophenylphosphate, a commonly employed RNA model) compared with Cu(II)–24. However, the increase in reactivity was modest in comparison to Cu(II)–trialkylated tacn complexes.<sup>44</sup> The role of the guanidinium arms in these complexes was largely confined to reducing formation of inactive dihydroxo-bridged dimers, rather than direct participation in cleavage. On the other hand,

incorporation of two ethyl-guanidinium pendants (**40**, Figure 8) resulted in a complex, Cu(II)–40, whose X-ray structure revealed unexpected coordination of the guanidine groups (Figure 10).<sup>44</sup> Speciation studies further confirmed that, under slightly basic conditions, guanidine saturates the Cu(II) coordination sphere, forming remarkably strong Cu–N(guanidine) bonds ( $\log K > 6.5$ ). The absence of “free” sites for complex–substrate interaction contributes to the inactivity of Cu(II)–40 toward BNPP and HPNPP. Interestingly, Cu(II)–40 and Cu(II)–41 do cleave supercoiled pBR 322 plasmid DNA, albeit at marginally increased rates compared with Cu(II)–24.<sup>44</sup> Solution speciation studies showed a

**Table 1.** First-order rate constants (pH 7) for the cleavage of activated model phosphate esters, BNPP and HPNPP, and single-strand DNA by a selection of Cu(II)-tacn-based complexes

compound	BNPP $k_{\text{obs}}$ ( $\times 10^{-6} \text{ s}^{-1}$ ) ( $T = 50 \text{ }^\circ\text{C}$ )	HPNPP $k_{\text{obs}}$ ( $\times 10^{-6} \text{ s}^{-1}$ ) ( $T = 25 \text{ }^\circ\text{C}$ )	plasmid DNA $k_{\text{obs}}$ ( $\times 10^{-5} \text{ s}^{-1}$ ) ( $T = 37 \text{ }^\circ\text{C}$ )	refs
substrate only	0.0003	0.012(7)		42
Cu(II)-25	12.4			46
Cu(II)-26	63			47
Cu(II)-27	43		3.0	41
Cu(II)-28	14.3			45
Cu(II)-30	15.3			45
Cu(II)-31	70.1			46
Cu(II)-34	0.48(1)			45
Cu(II) <sub>2</sub> -35	5.2			19
Cu(II) <sub>2</sub> -36	0.86			19
Cu(II) <sub>2</sub> -38	24.3			17
Cu(II) <sub>2</sub> -39	1.1			17
Cu(II)-40	0.0100(3)	0.13(6)	1.58(5)	44
Cu(II)-41	72.4(8)	32(3)	2.53(4)	44
Cu(II)-42	1.65(3)	1.88(3)	$k_1^a = 27.1(3)$ $k_2^a = 1.2(5)$ $k_3^a = 11.2(5)$	42
Cu(II)-43	2.36(3)	2.74(2)	8(1)	42
Cu(II)-44	2.39(4)	2.30(3)	6.7(3)	42
Cu(II) <sub>2</sub> -45	1.35(9)	1.46(9)	13.0(1)	43
Cu(II)-46	7.0(1)	14(2)	18.7(2)	43
Cu(II)-47	10.2(9)	14.1(7)	5.51(3)	43
[Cu(tacn)(OH <sub>2</sub> ) <sub>2</sub> ] <sup>2+</sup>	1.71(1)	3.58(2)	1.2(4)	47

<sup>a</sup>Rates of cleavage of supercoiled DNA to relaxed circular form ( $k_1$ ) to linear form ( $k_2$ ) and to DNA oligomers ( $k_3$ ).

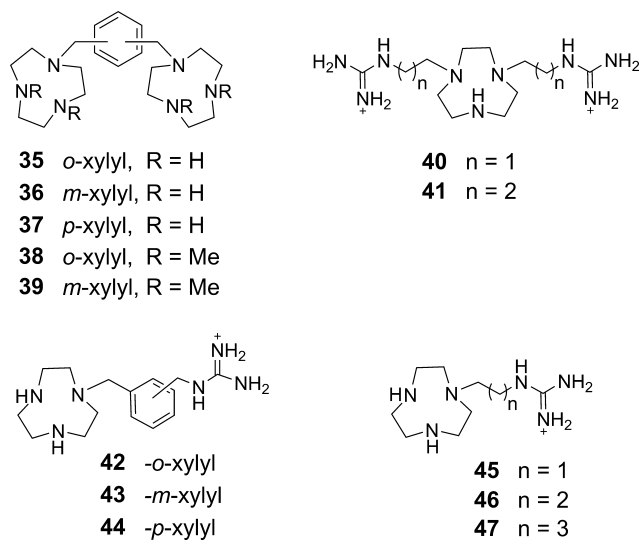


**Figure 8.** Binucleating (35–39) and guanidinium pendant-bearing tacn ligands (40–47) applied in phosphate ester hydrolysis.

complex distribution of species with multiple inactive mononuclear and polynuclear complexes present at pH 7.0. Guanidine coordination contributed to the poor activity of Cu(II)-40; displacement of this group is required for DNA binding and subsequent cleavage. Charge-assisted H-bonding interactions between the negatively charged phosphate groups

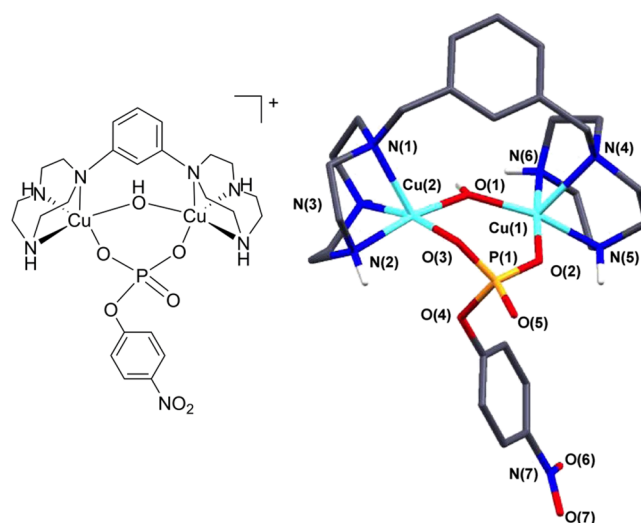


**Figure 9.** NPP-bridged binuclear complex, Cu(II)<sub>2</sub>-36-NPP. Adapted with permission from ref 1. Copyright 2012 Elsevier.

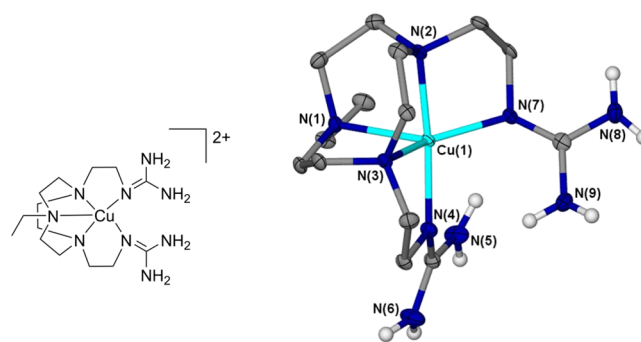


**Figure 10.** Guanidine coordination in Cu(II)-40. Adapted with permission from ref 44. Copyright 2010 American Chemical Society.

on the DNA backbone and guanidinium pendants was postulated to promote DNA phosphate–Cu(II) coordinative interactions and subsequent cleavage.

In comparison, cleavage of supercoiled DNA can be achieved at an increased rate if the guanidinium group is well-positioned to promote charge-assisted H-bonding interactions with neighboring phosphodiester groups (Figure 11). This is exemplified by fact that Cu(II)-42, Cu(II)-43, and Cu(II)-44, featuring single xylyl-guanidinium pendants, showed improved rates of supercoiled DNA cleavage (Table 1).<sup>42,43</sup>

In particular, the complex of the *o*-xylyl derivative, Cu(II)-42, exhibited a pseudo-first-order rate constant of  $2.7 \times 10^{-4} \text{ s}^{-1}$  at pH 7.0, 37 °C; 22-fold higher than that for Cu(II)-24. Interestingly, this complex represents a rare case where the sequential cleavage of supercoiled DNA (form I) to relaxed form II, to linear form III, and finally to DNA oligomers could be followed and rate constants determined for each transformation. Accumulation of relaxed form II to ~90% of the initial DNA concentration was observed due to the slow rate of cleavage of relaxed form II to linear form III, compared with the cleavage of either supercoiled DNA (form I) or linear form III.<sup>42</sup>

Similarly, incorporation of more flexible single alkyl-guanidinium pendants (45–47) improved the rate of BNPP and HPNPP cleavage. The greater flexibility of the pendant was postulated to assist cleavage by allowing better interaction of guanidinium groups with the Cu(II)-bound phosphate ester.

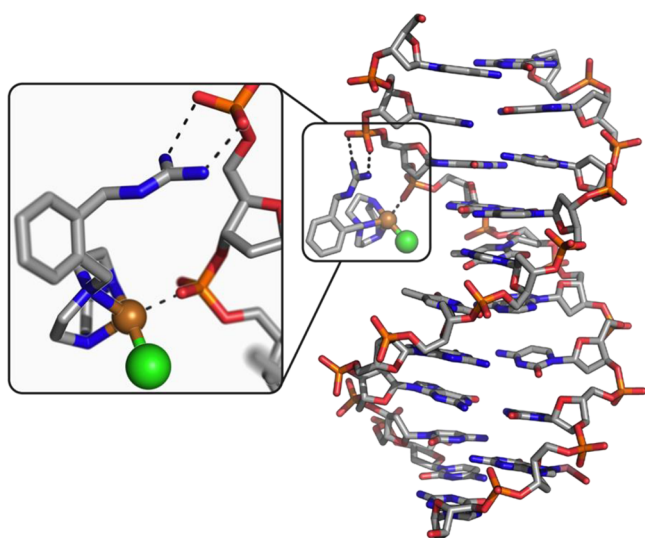


**Figure 11.** Plausible mode of interaction of Cu(II)-42 with DNA. Adapted with permission from ref 1. Copyright 2012 Elsevier.

These Cu(II) complexes also cleaved plasmid DNA at faster rates than Cu(II)-tacn and Cu(II)-tacn-bis(alkylguanidinium) complexes (Table 1),<sup>43</sup> suggesting that the Cu(II) centers and positively charged guanidinium group act in concert to improve DNA cleavage. Thus, cooperativity between metal ions and amino acid residues located within the active sites of natural metallo-nucleases may be mimicked to a degree by choosing spacers with suitable geometries. Moreover, as nicely demonstrated by Cu(II)-42, natural phosphate esters may not necessarily follow the reactivity patterns established for activated synthetic phosphate esters.

Introduction of charge or H-bonding groups has also yielded enhancements in activity for other ligands promoting structural reorganization of a metal center and an auxiliary unit to affect cooperative cleavage (Figure 12).<sup>1</sup> The DNA cleavage activity of Cu(II) complexes of 2,2'-bipyridine (bpy) derivatives

bearing electropositive pendants (48–54, Figure 12) was dependent on the relative bulk and rigidity of the pendant arms, as well as their position on the bpy backbone. These pendants can influence substrate binding through electrostatic or charge-assisted H-bonding interactions. Complexes Cu(II)-48, Cu(II)-50 and Cu(II)-53, bearing positively charged functionalities, showed almost 10-fold higher activities compared with the unmodified complex (pseudo-Michaelis–Menten parameter,  $k_{\text{cat}} = 1.23 \times 10^{-3}$ ,  $1.17 \times 10^{-3}$ , and  $1.15 \times 10^{-3} \text{ s}^{-1}$ , respectively, at pH 7.2 and 37 °C).<sup>1</sup> Similarly, Krämer and co-workers demonstrated the importance of H-bonding interactions in activation and stabilization of the transition state. The rate of BNPP cleavage by Cu(II)-55, featuring a ligand with tertiary amino groups on rigid alkyne pendants, was 1000-times faster relative to that of Cu(II)-56, the complex devoid of H-bond donors.<sup>1</sup> The tertiary amino groups were postulated to participate in H-bonding with the phosphate ester, leading to an increase in the rate of phosphodiester hydrolysis. Similarly, the *trans*-positioned  $\text{NH}_2$  group in Cu(II)-60 enhanced substrate binding through charge-assisted H-bonding, with this complex effectively cleaving plasmid DNA at pH 7.0 ( $k_{\text{obs}} = 5.5 \times 10^{-5} \text{ s}^{-1}$  at 35 °C).<sup>1</sup> Interestingly, Cu(II)-62 mediates plasmid DNA cleavage at an even faster rate ( $k_{\text{obs}} = 2.3 \times 10^{-3} \text{ s}^{-1}$ );<sup>1</sup> the improved hydrolytic activity being attributed to an increased affinity for DNA arising from interactions involving its hydroxyl groups.

Despite these efforts, the catalytic activity of synthetic nucleases remains well below that of natural enzymes. The main focus thus far has been on mimicking selected structural features of the metalloenzymes. However, the nonpolar nature of enzyme active sites also appears to be key to their extraordinarily high catalytic activities. Recent studies of the hydrolytic activity of metal complexes in organic solvents with a lower dielectric constant than water have yielded enhanced cleavage rates.<sup>1,48,50</sup> Synthetic nucleases featuring macrocyclic ligands linked to hydrophobic polymeric materials have been prepared in an attempt to mimic the nonpolar nature of enzyme active sites. However, the contribution of desolvation,

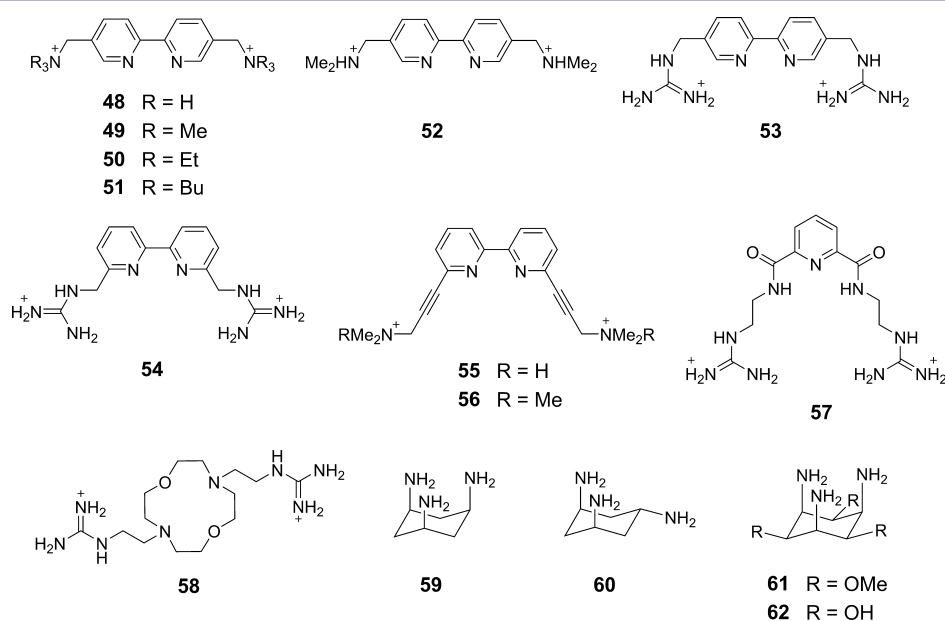


**Figure 12.** Examples of ligands featuring positively charged H-bond donors (guanidinium and ammonium pendants) applied in phosphate ester hydrolysis.<sup>1</sup>



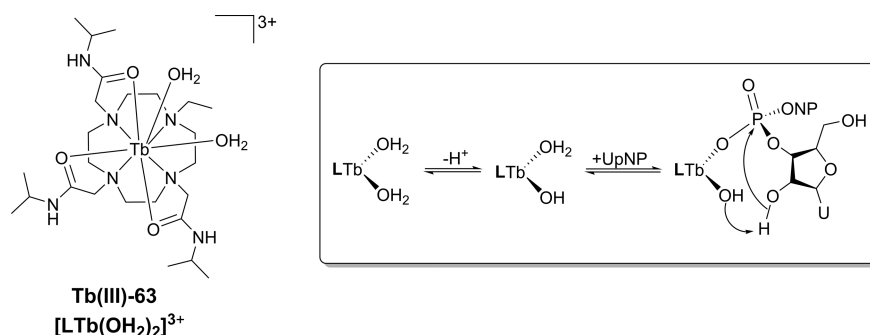


**Figure 13.** RNA-cleaving Tb(III)-63 complex and its proposed mechanism of UpNP cleavage.<sup>53</sup>

medium effects, and dispersion interactions remains considerably under-studied for synthetic nucleases. The challenge for chemists is to emulate such microenvironments in synthetic systems.

Careful manipulation of the metal coordination environment can also be used to develop synthetic nucleases for practical molecular biological applications. A coordinatively unsaturated Tb(III)–cyclen complex featuring three isopropylacetamide pendants, Tb(III)–63 (Figure 13), proved effective as a “footprinting” agent for mapping the binding site of drugs to therapeutically significant folded RNA motifs.<sup>53</sup> By restricting the number of amide pendants in Tb(III)–63 to three, two labile metal coordination sites were provided for substrate binding and aqua ligand-assisted deprotonation of the 2'-OH group to generate a more potent nucleophile. We first examined the function of the complex as a synthetic ribonuclease using an RNA model, uridine-3'-*p*-nitrophenyl-phosphate (UpNP). The complex accelerates UpNP cleavage by 100-fold above the background rate ( $k_{\text{obs}} = 0.055(1) \text{ s}^{-1}$  at 21 °C and pH 7.5; apparent second-order rate constant of  $277(5) \text{ M}^{-1} \text{ s}^{-1}$ ). When incubated with short RNA constructs (HIV TAR, HIV DIS, and ribosomal A-site) and formyl methionine tRNA, the complex exclusively cleaves at the more solvent-exposed single-stranded “bulge” regions of these motifs. It was subsequently used to detect the interaction of the HIV-I transactivation response (TAR) mRNA element with two known binders, the Tat peptide and neomycin B.<sup>53</sup>

## ■ SENSORS FOR BIOMOLECULES

Ligand coordination flexibility in “coordinatively unsaturated” azamacrocyclic metal complexes is a clear advantage for designing responsive systems for biomolecule detection, permitting the analyte of interest to bind to the metal ion by displacing coordinated water (or solvent) molecules. Upon binding, the analyte induces changes in the metal coordination environment that can be detected by one or more analytical methods. DNA nucleobase-selective recognition by azamacrocyclic complexes was first investigated by Kimura and co-workers.<sup>54</sup> The Zn(II) ion forms a strong coordinate bond with an imido anion, allowing the recognition of thymine and uracil bases by Zn(II)–cyclen complexes in aqueous solution at physiological pH.<sup>54</sup> This strong M(II)–mido interaction can also be exploited for electrochemical recognition of molecules using ferrocene-based Cu(II)– and Zn(II)–cyclen systems.

Initially, we applied a cyclen ligand featuring a ferrocene (Fc) pendant to demonstrate the binding of nitrate to its Cu(II) complex, Cu(II)–64, and recognition of thymine and related nucleosides by the Zn(II) complex, Zn(II)–64 (Figure 14).<sup>55,56</sup>

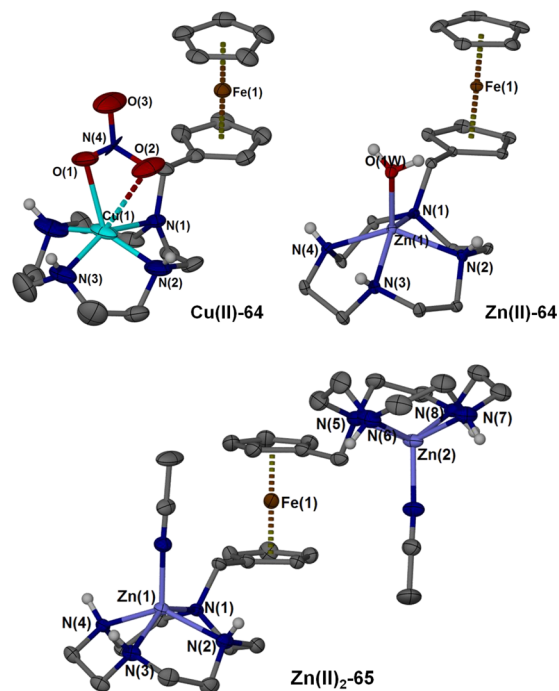


**Figure 14.** Ferrocene (Fc)-bearing M(II)–cyclen receptor complexes. Adapted with permission from refs 55–57. Copyright 2007 American Chemical Society and 2009 John Wiley and Sons.

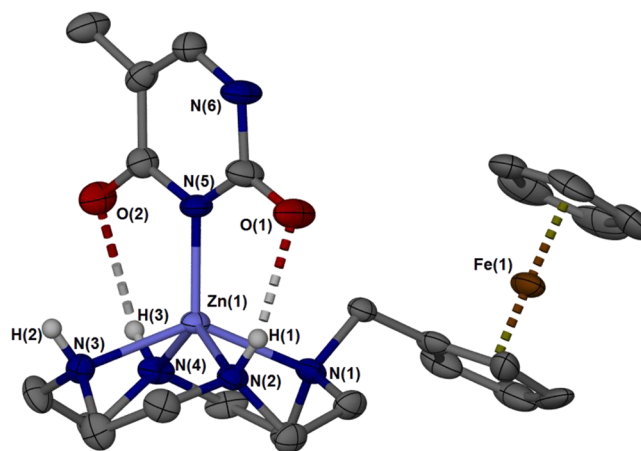


**Figure 15.** Zn(II)-64–thymine (1:1) complex. Adapted with permission from ref 56. Copyright 2007 American Chemical Society.

The attachment of a Fc moiety to the cyclen framework provided a redox signaling unit (Zn(II)–64, Figure 14). Our

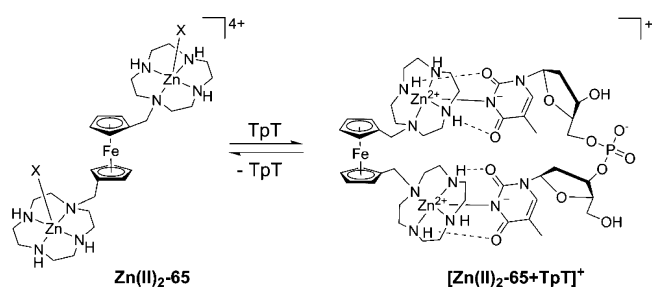


**Figure 16.** Proposed mode of binding of TpT by the  $\text{Zn(II)}_2\text{-65}$ .<sup>57</sup>

electrochemical studies of the interaction of  $\text{Zn(II)}_2\text{-64}$  with thymine and its derivatives, thymidine (dT) and thymidine-5'-monophosphate ( $\text{TMP}^{2-}$ ), revealed a small shift of  $-10$  mV when excess thymine was added to  $\text{Zn(II)}_2\text{-64}$  in acetonitrile.<sup>56</sup> In aqueous solution at physiological pH, similar subtle

voltammetric responses were observed on addition of dT and  $\text{TMP}^{2-}$ . The binding of thymine and its derivatives to zinc(II) was confirmed by X-ray crystallography, NMR, and IR spectroscopy. The X-ray structure of the  $\text{Zn(II)}$ –cyclen–thymine adduct showed that the deprotonated anionic thymine coordinates (Figure 15).<sup>56</sup> As noted previously, H-bonding between the thymine amido oxygens and two macrocycle amines increases the strength of binding.<sup>54,56</sup>

The sensitivity can be improved by linking two  $\text{Zn(II)}$ –cyclen units via a Fc group. Thus, we found  $\text{Zn(II)}_2\text{-65}$  (Figure 16) to be remarkably selective for thymidyl(3'-5')thymidine (TpT) relative to other nucleotides.<sup>57</sup> A shift of  $-36$  mV in the Fc moiety redox potential was observed on addition of 1 equiv of TpT. Interestingly, the negative shift in potential remained almost unaffected on addition of excess thymine or TMP, indicating a remarkably high affinity of TpT for  $\text{Zn(II)}_2\text{-65}$ . A 1:1 binding stoichiometry was determined

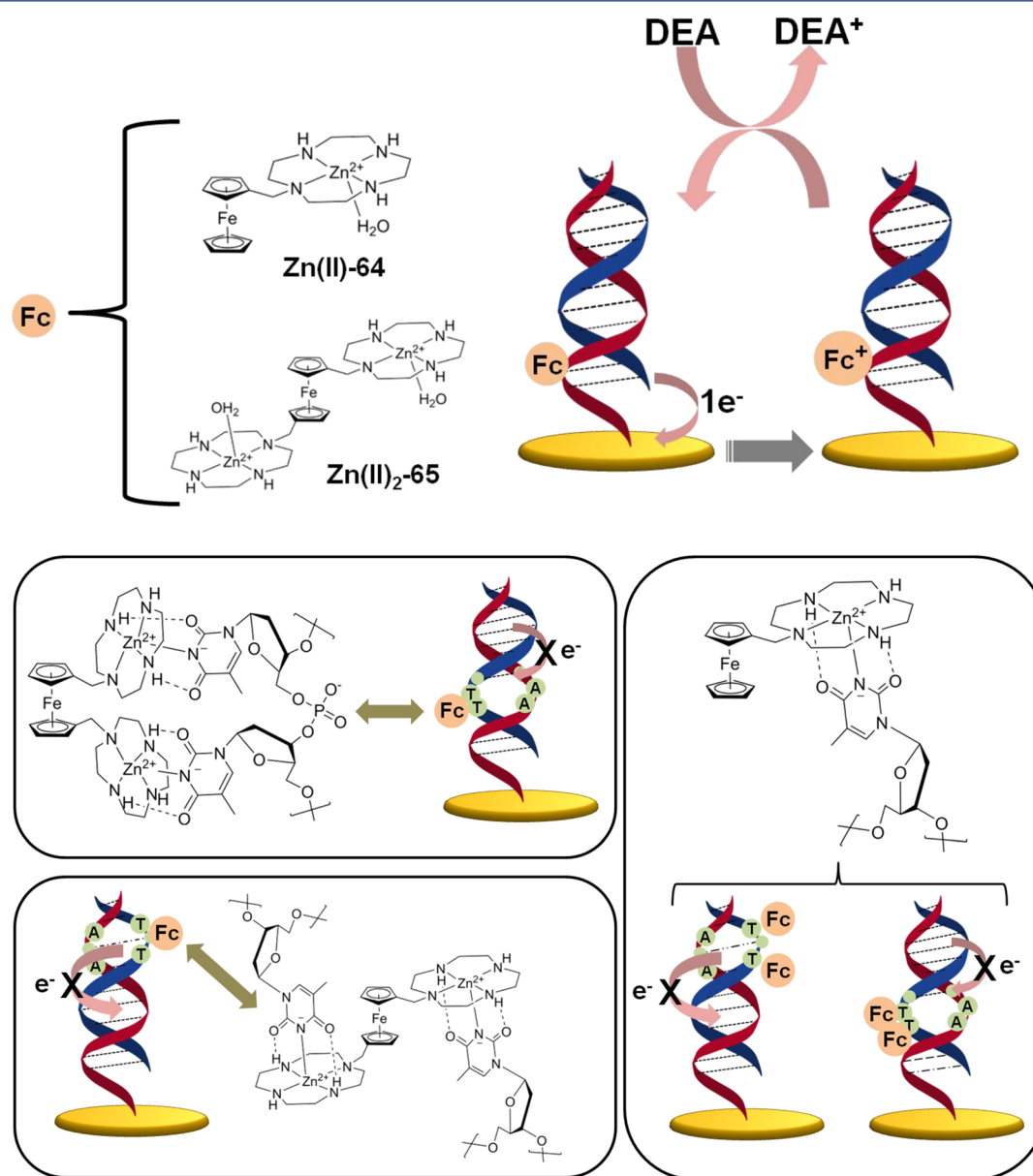


**Figure 17.** Electrocatalytic oxidation of diethylamine (DEA) by  $\text{Zn(II)}_2\text{-64}$  and  $\text{Zn(II)}_2\text{-65}$  at a DNA-modified gold electrode surface and their mode of interaction with duplex DNA. Adapted with permission from ref 58. Copyright 2010 American Chemical Society.

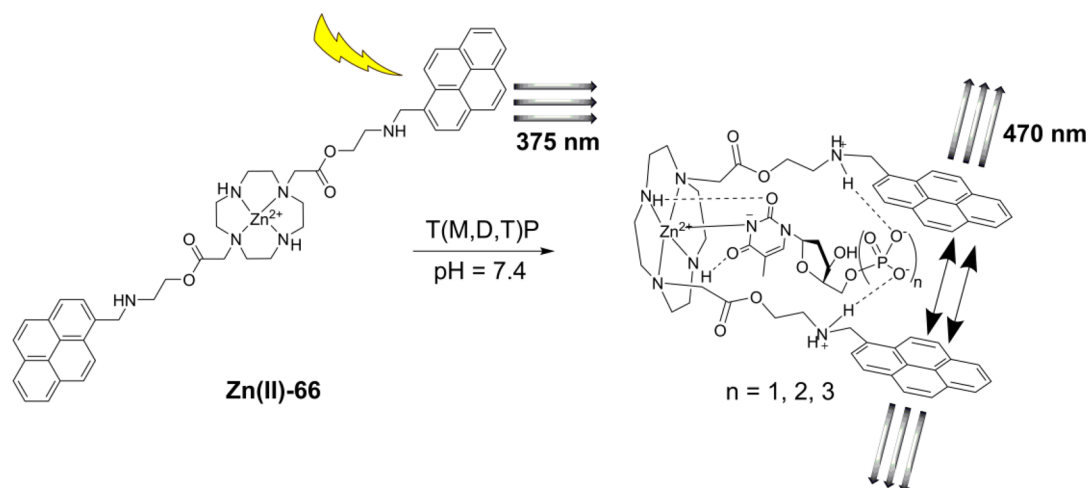


Figure 18. Proposed mode of interaction of the Zn(II)-66 with thymidine phosphates.<sup>59</sup>

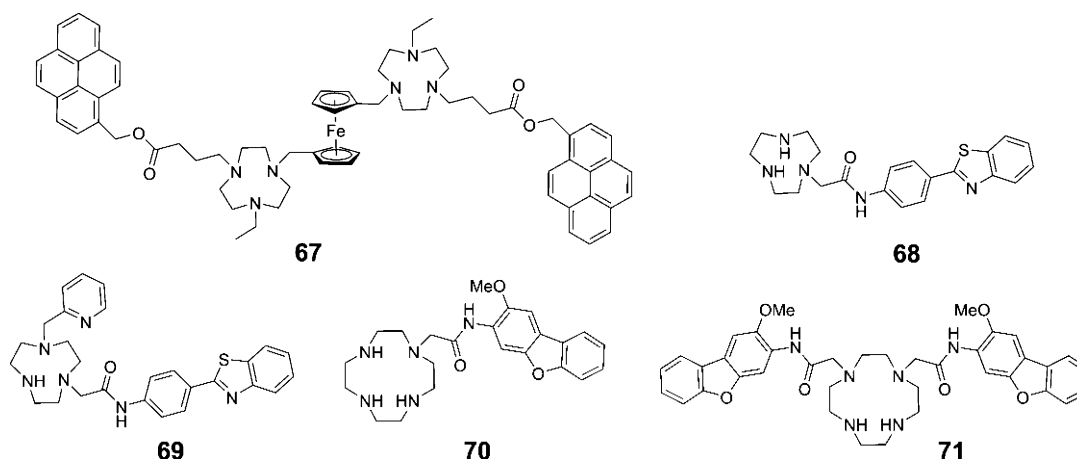


Figure 19. Examples of fluorophore-functionalized ligands 67–71.

electrochemically and via UV/vis spectrophotometric titrations ( $K_{\text{app}} = 0.89(1) \times 10^6 \text{ M}^{-1}$ ).<sup>57</sup> A two-point binding model for formation of the receptor–TpT adduct,  $[\text{Zn}(\text{II})_2\text{-65} + \text{TpT}]^+$ , was proposed, in which a major structural rearrangement occurs, yielding a macrochelate that bridges the two Zn(II) centers (Figure 16).<sup>57</sup> This model draws support from similar findings by Kimura and co-workers for a *p*-xylyl bridged bis(Zn(II)–cyclen) complex.<sup>54,57</sup>

As a logical extension, we then developed a highly sensitive electrochemical sensor for DNA hybridization based on Fc-bearing Zn–cyclen complexes, which provided a viable alternative to enzyme and nanocatalyst-based electrochemical methods. The high affinity of these complexes for thymine bases and TpT groups, duplex-mediated charge transfer in DNA, and electrocatalytic oxidation of diethylamine, were used in combination to develop an assay that allows the selective discrimination of complementary, noncomplementary, and single-base mismatches in DNA sequences with subpicomolar detection limits (Figure 17).<sup>58</sup>

The Zn(II)–imido anion interaction can also be used in the fluorescence-based detection of thymidine mono-, di-, and triphosphate nucleotides (TMP, TDP, and TTP) by a Zn(II)–cyclen complex containing two pyrene pendants (Zn(II)–66, Figure 18).<sup>59</sup> Their binding induces conformational changes that align the pyrene units of the receptor and enhance excimer emission at 470 nm at the expense of monomer emission. From

NMR titration experiments, we confirmed a 1:1 binding stoichiometry for each guest molecule. The receptor showed some selectivity for TTP over the other nucleotides, and an apparent binding constant of  $3.2(3) \times 10^5 \text{ M}^{-1}$  was determined at pH 7.4 in 1:9  $\text{CH}_3\text{CN}/\text{HEPES}$ .<sup>59</sup>

Pyrene, benzofuran, and benzothiazole chromophores can also be used to build other tacn- and cyclen-based ligands capable of the fluorescence-based sensing of selected analytes (representative examples from our own work are shown in Figure 19).<sup>60–62</sup> Notably, Zn(II)<sub>2</sub>–67, a complex incorporating one Fc unit and two pyrene units, is a good example of a receptor for biological phosphate anions. Dual-mode electrochemical and fluorescence-based detection of polyphosphate anions, such as PPI, ATP and ADP, was achieved with this receptor.<sup>62</sup> Binding of the polyphosphates induces a conformational rearrangement, which forces the pyrene units to the same side of Fc unit. This enhances pyrene excimer emission and shifts the electrochemical potential of the Fc/Fc<sup>+</sup> couple.

The strength of the Zn(II)–imido and Zn(II)–phosphate interactions is key to the high detection sensitivities of Zn–cyclen-based systems. To work as selective reporter molecules, however, the response should remain unaffected by the presence of other species (particularly other phosphate-bearing molecules), even at very low analyte concentrations. A major challenge that restricts the practical applications of such Zn(II)–cyclen-based electrochemical and fluorescent chemo-

sensors and needs to be tackled through innovative design and synthesis is the lack of an exclusively selective response. Our findings, however, point toward the possibility of developing more specific receptors in the future. One way to achieve this could be through synthetic designs incorporating functionalities to further increase the affinity toward a specific phosphate or nucleotide via complementary H-bonding interactions.

## CONCLUDING REMARKS

In this Account, the potential of metal complexes of tacn- and cyclen-based macrocyclic ligands to be exploited as structural metalloprotein models, nuclease mimics, and nucleobase sensors has been highlighted. Critical to these applications, “coordinative unsaturation” allows for reversible binding of substrate molecules via the formation and dissociation of coordination bonds.

With regards to the mimicry of metalloproteases, our studies have generated a number of tacn-based Cu(II) complexes that exhibit a degree of cooperativity between either multiple metal centers in proximity or a metal center and a charged ancillary group in accelerating the rate of cleavage of a number of phosphate esters. While these systems are still orders of magnitude less active than enzymes such as alkaline phosphatase, they nonetheless capture aspects of the catalytic cycle of these natural systems.

The utility of macrocyclic metal complexes as biosensors is evidenced by our development of ferrocene- and pyrene-bearing Zn(II)–cyclen complexes as single- and dual-mode electrochemical and fluorescence-based sensors for imide-containing nucleobase derivatives, as well as a highly sensitive method for DNA sequence mismatch detection. Further research could result in probes suitable for use in a clinical diagnostic setting.

## AUTHOR INFORMATION

### Corresponding Authors

\*E-mail: [tanmaya.joshi@monash.edu](mailto:tanmaya.joshi@monash.edu).

\*E-mail: [bim.graham@monash.edu](mailto:bim.graham@monash.edu).

\*E-mail: [leone.spiccia@monash.edu](mailto:leone.spiccia@monash.edu).

### Funding

We are grateful to the Australian Research Council for Discovery Project funding, a Discovery Outstanding Researcher Award (L.S.), and a Future Fellowship (B.G.).

### Notes

The authors declare no competing financial interest.

### Biographies

**Tanmaya Joshi** (Ph.D., Monash University) is currently a senior postdoctoral fellow in the groups of Prof. Spiccia and Dr. Graham. His research focuses on integrating coordination chemistry and nanomaterials to develop metal-based imaging, therapeutic, and diagnostic agents.

**Bim Graham** (Ph.D., Monash University) is currently a senior lecturer within the Monash Institute of Pharmaceutical Sciences. His group's research focuses on the development of chemical tools to probe biological systems via fluorescence, NMR, and EPR-based techniques.

**Leone Spiccia** (Ph.D., University of Western Australia) is currently Professor of Chemistry at Monash University. His research focuses on the development of metal complexes and inorganic materials for applications that include solar energy conversion, therapeutics, and biosensors.

## REFERENCES

- (1) Desbouis, D.; Troitsky, I. P.; Belousoff, M. J.; Spiccia, L.; Graham, B. Copper(II), zinc(II) and nickel(II) complexes as nuclease mimetics. *Coord. Chem. Rev.* **2012**, *256*, 897–937 and references therein.
- (2) Shinoda, S. Dynamic cyclen-metal complexes for molecular sensing and chirality signaling. *Chem. Soc. Rev.* **2013**, *42*, 1825–1835.
- (3) Lindoy, L. F.; Park, K.-M.; Lee, S. S. Metals, macrocycles and molecular assemblies - macrocyclic complexes in metallo-supramolecular chemistry. *Chem. Soc. Rev.* **2013**, *42*, 1713–1727.
- (4) Kimura, E.; Kikuta, E. Why zinc in zinc enzymes? From biological roles to DNA base-selective recognition. *J. Biol. Inorg. Chem.* **2000**, *5*, 139–155.
- (5) Geduhn, J.; Walenzyk, T.; Konig, B. Transition metal complexes of some azamacrocycles and their use in molecular recognition. *Curr. Org. Synth.* **2007**, *4*, 390–412.
- (6) Shokeen, M.; Anderson, C. J. Molecular Imaging of Cancer with Copper-64 Radiopharmaceuticals and Positron Emission Tomography (PET). *Acc. Chem. Res.* **2009**, *42*, 832–841.
- (7) Reichert, D. E.; Lewis, J. S.; Anderson, C. J. Metal complexes as diagnostic tools. *Coord. Chem. Rev.* **1999**, *184*, 3–66.
- (8) Bünzli, J.-C. G. Lanthanide luminescence for biomedical analyses and imaging. *Chem. Rev.* **2010**, *110*, 2729–2755.
- (9) Montgomery, C. P.; Murray, B. S.; New, E. J.; Pal, R.; Parker, D. Cell-penetrating metal complex optical probes: targeted and responsive systems based on lanthanide luminescence. *Acc. Chem. Res.* **2009**, *42*, 925–937 and references therein.
- (10) Gloe, K. *Macrocyclic Chemistry: Current Trends and Future Perspectives*; Springer: Dordrecht, the Netherlands, 2005; and references therein.
- (11) Atkins, T. J. Tricyclic trisaminomethanes. *J. Am. Chem. Soc.* **1980**, *102*, 6364–6365.
- (12) Weisman, G. R.; Johnson, V.; Fiala, R. E. Tricyclic orthoamides: Effects of lone-pair orientation upon NMR spectra. *Tetrahedron Lett.* **1980**, *21*, 3635–3638.
- (13) Blake, A. J.; Fallis, I. A.; Parsons, S.; Ross, S. A.; Schroder, M. Asymmetric functionalisation of aza macrocycles. Syntheses, crystal structures and electrochemistry of [Ni(Bz[9]aneN<sub>3</sub>)<sub>2</sub>][PF<sub>6</sub>]<sub>2</sub> and [Pd(Bz[9]aneN<sub>3</sub>)<sub>2</sub>][PF<sub>6</sub>]<sub>2</sub>·2MeCN (Bz[9]aneN<sub>3</sub>= 1-benzyl-1,4,7-triazacyclononane). *J. Chem. Soc., Dalton Trans.* **1996**, 525–532.
- (14) Warden, A. C.; Spiccia, L.; Hearn, M. T. W.; Boas, J. F.; Pilbrow, J. R. The synthesis, structure and properties of copper(II) complexes of asymmetrically functionalized derivatives of 1,4,7-triazacyclononane. *Dalton Trans.* **2005**, 1804–1813.
- (15) Warden, A.; Graham, B.; Hearn, M. T. W.; Spiccia, L. Synthesis of novel derivatives of 1,4,7-triazacyclononane. *Org. Lett.* **2001**, *3*, 2855–2858.
- (16) Belousoff, M. J.; Graham, B.; Spiccia, L. Copper(II) complexes of N-methylated derivatives of ortho- and meta-xylyl-bridged bis(1,4,7-triazacyclononane) ligands: synthesis, X-ray structure and reactivity as artificial nucleases. *Eur. J. Inorg. Chem.* **2008**, *2008*, 4133–4139.
- (17) Belousoff, M. J.; Graham, B.; Moubaraki, B.; Murray, K. S.; Spiccia, L. Oxalato-bridged dinuclear copper(II) complexes of N-alkylated derivatives of 1,4,7-triazacyclononane: synthesis, X-ray crystal structures and magnetic properties. *Eur. J. Inorg. Chem.* **2006**, *2006*, 4872–4878.
- (18) Battle, A. R.; Graham, B.; Spiccia, L.; Moubaraki, B.; Murray, K. S.; Skelton, B. W.; White, A. H. Structure and magnetic properties of polynuclear chloro- and hydroxo-bridged copper(II) complexes formed by a tetramacrocyclic derivative of 1,4,7-triazacyclononane. *Inorg. Chim. Acta* **2006**, *359*, 289–297.
- (19) Fry, F. H.; Spiccia, L.; Jensen, P.; Moubaraki, B.; Murray, K. S.; Tiekink, E. R. T. Binuclear copper(II) complexes of xylyl-bridged bis(1,4,7-triazacyclononane) ligands. *Inorg. Chem.* **2003**, *42*, 5594–5603.
- (20) Fry, F. H.; Moubaraki, B.; Murray, K. S.; Spiccia, L.; Warren, M.; Skelton, B. W.; White, A. H. Asymmetry in endogenously bridged binuclear copper(II) and zinc(II) complexes formed by 1,2-bis[1,4,7-triazacyclonon-1-yl]propan-2-ol. *Dalton Trans.* **2003**, 866–871.

- (21) Fry, F. H.; Jensen, P.; Kepert, C. M.; Spiccia, L. Macrocyclic copper(II) and zinc(II) complexes incorporating phosphate esters. *Inorg. Chem.* **2003**, *42*, 5637–5644.
- (22) Graham, B.; Spiccia, L.; Fallon, G. D.; Hearn, M. T. W.; Mabbs, F. E.; Moubaraki, B.; Murray, K. S. Structure and magnetic properties of tri- and hexa-nuclear hydroxo-bridged copper(II) complexes formed by a trimacrocyclic derivative of 1,4,7-triazacyclononane. *J. Chem. Soc., Dalton Trans.* **2002**, 1226–1232.
- (23) Graham, B.; Hearn, M. T. W.; Junk, P. C.; Kepert, C. M.; Mabbs, F. E.; Moubaraki, B.; Murray, K. S.; Spiccia, L. Syntheses, crystal structures, magnetic properties, and EPR spectra of tetranuclear copper(II) complexes featuring pairs of “roof-shaped”  $\text{Cu}_2\text{X}_2$  dimers with hydroxide, methoxide, and azide bridges. *Inorg. Chem.* **2001**, *40*, 1536–1543.
- (24) Graham, B.; Grannas, M. J.; Hearn, M. T. W.; Kepert, C. M.; Spiccia, L.; Skelton, B. W.; White, A. H. Coordination chemistry of a novel tetramacrocyclic ligand derived from 1,4,7-triazacyclononane: synthesis, structure, and properties of nickel(II) and copper(II) complexes. *Inorg. Chem.* **2000**, *39*, 1092–1099.
- (25) Brudenell, S. J.; Spiccia, L.; Bond, A. M.; Comba, P.; Hockless, D. C. R. Structural, EPR, and electrochemical studies of binuclear copper(II) complexes of bis(pentadentate) ligands derived from bis(1,4,7-triazacyclononane) macrocycles. *Inorg. Chem.* **1998**, *37*, 3705–3713.
- (26) Spiccia, L.; Graham, B.; Hearn, M. T. W.; Lazarev, G.; Moubaraki, B.; Murray, K. S.; Tiekink, E. R. T. Towards synthetic models for trinuclear copper active sites of ascorbate oxidase and laccase: self-assembly, crystal structure and magnetic properties of the copper(II) complexes of 1,3,5-tris(1,4,7-triazacyclonon-1-ylmethyl)-benzene. *J. Chem. Soc., Dalton Trans.* **1997**, 4089–4098.
- (27) Graham, B.; Fallon, G. D.; Hearn, M. T. W.; Hockless, D. C. R.; Lazarev, G.; Spiccia, L. Coordination modes of a series of xylylene-bridged bis(1,4,7-triazacyclonon-1-yl) ligands: synthesis, structure, and properties of nickel(II) and copper(II) complexes. *Inorg. Chem.* **1997**, *36*, 6366–6373.
- (28) Brudenell, S. J.; Spiccia, L.; Tiekink, E. R. T. Binuclear copper(II) complexes of bis(pentadentate) ligands derived from alkyl-bridged bis(1,4,7-triazacyclononane) macrocycles. *Inorg. Chem.* **1996**, *35*, 1974–1979.
- (29) Solomon, E. I.; Sundaram, U. M.; Machonkin, T. E. Multicopper oxidases and oxygenases. *Chem. Rev.* **1996**, *96*, 2563–2606 and references therein.
- (30) Tolman, W. B. Making and breaking the dioxygen O–O bond: new insights from studies of synthetic copper complexes. *Acc. Chem. Res.* **1997**, *30*, 227–237 and references therein.
- (31) Messerschmidt, A.; Luecke, H.; Huber, R. X-ray structures and mechanistic implications of three functional derivatives of ascorbate oxidase from zucchini: reduced, peroxide and azide forms. *J. Mol. Biol.* **1993**, *230*, 997–1014.
- (32) Adams, H.; Bailey, N. A.; Dwyer, M. J. S.; Fenton, D. E.; Hellier, P. C.; Hempstead, P. D.; Latour, J. M. Synthesis and crystal structure of a first-generation model for the trinuclear copper site in ascorbate oxidase and of a dinuclear silver precursor. *J. Chem. Soc., Dalton Trans.* **1993**, 1207–1216.
- (33) Karlin, K. D.; Gan, Q. F.; Farooq, A.; Liu, S.; Zubieta, J. A trinuclear copper(I) complex: reaction with dioxygen and the formation of a hexanuclear copper(II) cluster. *Inorg. Chem.* **1990**, *29*, 2549–2551.
- (34) Chaudhuri, P.; Karpenstein, I.; Winter, M.; Butzlaff, C.; Bill, E.; Trautwein, A. X.; Florke, U.; Haupt, H.-J. Isolation of a spin-frustrated imidazolate-bridged trinuclear copper(II) complex potentially relevant to the multicopper oxidases. *J. Chem. Soc., Chem. Commun.* **1992**, 321–322.
- (35) Meenakumari, S.; Tiwary, S. K.; Chakravarty, A. R. Synthesis, crystal structure, and magnetic properties of a ferromagnetically coupled angular trinuclear copper(II) complex  $[\text{Cu}_3(\text{O}_2\text{CMe})_4(\text{bpy})_3(\text{H}_2\text{O})](\text{PF}_6)_2$ . *Inorg. Chem.* **1994**, *33*, 2085–2089.
- (36) Cao, R.; Müller, P.; Lippard, S. J. Tripodal tris-tacn and tris-dpa platforms for assembling phosphate-templated trimetallic centers. *J. Am. Chem. Soc.* **2010**, *132*, 17366–17369.
- (37) Vallee, B. L.; Auld, D. S. New perspective on zinc biochemistry: Cocatalytic sites in multi-zinc enzymes. *Biochemistry* **1993**, *32*, 6493–6500.
- (38) Mirica, L. M.; Stack, T. D. P. A tris( $\mu$ -hydroxy)tricopper(II) complex as a model of the native intermediate in Laccase and its relationship to a binuclear analogue. *Inorg. Chem.* **2005**, *44*, 2131–2133.
- (39) Mimmi, M. C.; Gullotti, M.; Santagostini, L.; Battaini, G.; Monzani, E.; Pagliarin, R.; Zoppellaro, G.; Casella, L. Models for biological trinuclear copper clusters. Characterization and enantioselective catalytic oxidation of catechols by the copper(II) complexes of a chiral ligand derived from (S)-(–)-1,1'-binaphthyl-2,2'-diamine. *Dalton Trans.* **2004**, 2192–2201.
- (40) Hough, E.; Hansen, L. K.; Birknes, B.; Jynge, K.; Hansen, S.; Hordvik, A.; Little, C.; Dodson, E.; Derewenda, Z. High-resolution (1.5 Å) crystal structure of phospholipase C from *Bacillus cereus*. *Nature* **1989**, *338*, 357–360.
- (41) Hegg, E. L.; Burstyn, J. N. Toward the development of metal-based synthetic nucleases and peptidases: a rationale and progress report in applying the principles of coordination chemistry. *Coord. Chem. Rev.* **1998**, *173*, 133–165 and references therein.
- (42) Tjioe, L.; Meininger, A.; Joshi, T.; Spiccia, L.; Graham, B. Efficient plasmid DNA cleavage by copper(II) complexes of 1,4,7-triazacyclononane ligands featuring xylyl-linked guanidinium groups. *Inorg. Chem.* **2011**, *50*, 4327–4339.
- (43) Tjioe, L.; Joshi, T.; Forsyth, C. M.; Moubaraki, B.; Murray, K. S.; Brugger, J.; Graham, B.; Spiccia, L. Phosphodiester cleavage properties of copper(II) complexes of 1,4,7-triazacyclononane ligands bearing single alkyl guanidine pendants. *Inorg. Chem.* **2012**, *51*, 939–953.
- (44) Tjioe, L.; Joshi, T.; Brugger, J. I.; Graham, B.; Spiccia, L. Synthesis, structure, and DNA cleavage properties of copper(II) complexes of 1,4,7-triazacyclononane ligands featuring pairs of guanidine pendants. *Inorg. Chem.* **2011**, *50*, 621–635.
- (45) Belousoff, M. J.; Battle, A. R.; Graham, B.; Spiccia, L. Syntheses, structures and hydrolytic properties of copper(II) complexes of asymmetrically N-functionalised 1,4,7-triazacyclononane ligands. *Polyhedron* **2007**, *26*, 344–355.
- (46) Belousoff, M. J.; Duriska, M. B.; Graham, B.; Batten, S. R.; Moubaraki, B.; Murray, K. S.; Spiccia, L. Synthesis, X-ray crystal structures, magnetism, and phosphate ester cleavage properties of copper(II) complexes of N-substituted derivatives of 1,4,7-triazacyclononane. *Inorg. Chem.* **2006**, *45*, 3746–3755.
- (47) Fry, F. H.; Fischmann, A. J.; Belousoff, M. J.; Spiccia, L.; Brügger, J. Kinetics and mechanism of hydrolysis of a model phosphate diester by  $[\text{Cu}(\text{Me}_3\text{tacn})(\text{OH})_2]^{2+}$  ( $\text{Me}_3\text{tacn}$  = 1,4,7-trimethyl-1,4,7-triazacyclononane). *Inorg. Chem.* **2005**, *44*, 941–950.
- (48) Hay, R. W.; Govan, N.; Norman, P. R. Kinetic and mechanistic studies of the reaction of a range of bases and metal-hydroxo complexes with the phosphonate ester 2,4-dinitrophenyl ethyl methylphosphonate in aqueous solution. *Transition Met. Chem.* **1998**, *23*, 133–138.
- (49) Hay, R. W.; Govan, N. The  $[\text{Cu}(\text{[9]aneN}_3)(\text{OH})(\text{OH}_2)]^+$  catalysed hydrolysis of the phosphotriester 2,4-dinitrophenyl diethyl phosphate ( $[\text{9]aneN}_3$  = 1,4,7-triazacyclononane). *Polyhedron* **1998**, *17*, 463–468.
- (50) Morrow, J. R. Speed limits for artificial ribonucleases. *Comments Inorg. Chem.* **2008**, *29*, 169–188.
- (51) Morrow, J. R.; Iranzo, O. Synthetic metallonucleases for RNA cleavage. *Curr. Opin. Chem. Biol.* **2004**, *8*, 192–200.
- (52) Hay, R. W. In *Handbook of Metal-Ligand Interactions in Biological Fluids: Bioinorganic Chemistry*; Berthon, G., Ed.; Marcel Dekker: New York, 1995; Vol. 1, pp 295–316.
- (53) Belousoff, M. J.; Ung, P.; Forsyth, C. M.; Tor, Y.; Spiccia, L.; Graham, B. New macrocyclic terbium(III) complex for use in RNA footprinting experiments. *J. Am. Chem. Soc.* **2009**, *131*, 1106–1114.

(54) Aoki, S.; Kimura, E. Zinc–nucleic acid interaction. *Chem. Rev.* **2004**, *104*, 769–788 and references therein.

(55) Gasser, G.; Belousoff, M. J.; Bond, A. M.; Spiccia, L. Binding of nitrate to a Cu(II)–cyclen complex bearing a ferrocenyl pendant: synthesis, solid-state X-ray structure, and solution-phase electrochemical and spectrophotometric studies. *Inorg. Chem.* **2007**, *46*, 3876–3888.

(56) Gasser, G.; Belousoff, M. J.; Bond, A. M.; Kosowski, Z.; Spiccia, L. Recognition of thymine and related nucleosides by a Zn(II)-cyclen complex bearing a ferrocenyl pendant. *Inorg. Chem.* **2007**, *46*, 1665–1674.

(57) Zeng, Z.; Torriero, A. A. J.; Belousoff, M. J.; Bond, A. M.; Spiccia, L. Synthesis, X-ray structure of ferrocene bearing bis(Zn-cyclen) complexes and the selective electrochemical sensing of TpT. *Chem. Eur. J.* **2009**, *15*, 10988–10996.

(58) Shiddiky, M. J. A.; Torriero, A. A. J.; Zeng, Z.; Spiccia, L.; Bond, A. M. Highly selective and sensitive DNA assay based on electrocatalytic oxidation of ferrocene bearing zinc(II)–cyclen complexes with diethylamine. *J. Am. Chem. Soc.* **2010**, *132*, 10053–10063.

(59) Zeng, Z.; Spiccia, L. Off–On fluorescent detection of thymidine nucleotides by a zinc(II)–cyclen complex bearing two diagonal pyrenes. *Chem. Eur. J.* **2009**, *15*, 12941–12944.

(60) Barreto, J.; Joshi, T.; Venkatachalam, T. K.; Reutens, D. C.; Graham, B.; Spiccia, L. Coordination chemistry of a mono-dibenzofuran derivative of 1,4,7,10-tetraazacyclododecane. *J. Coord. Chem.* **2015**, *68*, 335–349.

(61) Barreto, J.; Venkatachalam, T. K.; Joshi, T.; Kreher, U.; Forsyth, C. M.; Reutens, D.; Spiccia, L. Synthesis, characterization and coordination chemistry of aminophenylbenzothiazole substituted 1,4,7-triazacyclononane macrocycles. *Polyhedron* **2013**, *52*, 128–138.

(62) Zeng, Z.; Torriero, A. A. J.; Bond, A. M.; Spiccia, L. Fluorescent and electrochemical sensing of polyphosphate nucleotides by ferrocene functionalised with two Zn(II) (tacn) (pyrene) complexes. *Chem. Eur. J.* **2010**, *16*, 9154–9163.